Measurement report: Characteristics of nitrogen-containing organics in PM$_{2.5}$ in Urumqi, northwest China: differential impacts of combustion of fresh and old-age biomass materials

Yi-Jia Ma[1], Yu Xu[2,*], Ting Yang[1], Hong-Wei Xiao[2], Hua-Yun Xiao[2]

[1]School of Environmental Science and Engineering, Shanghai Jiao Tong University, Shanghai 200240, China

[2]School of Agriculture and Biology, Shanghai Jiao Tong University, Shanghai 200240, China

*Corresponding authors

Yu Xu

E-mail: xuyu360@sjtu.edu.cn

Abstract: Nitrogen-containing organic compounds (NOCs) are abundant and important aerosol components deeply involved in the global nitrogen cycle. However, the sources and formation processes of NOCs remain largely unknown, particularly in the city (Urumqi, China) farthest from the ocean worldwide. Here, NOCs in $PM_{2.5}$ collected in Urumqi over a one-year period were characterized by ultrahigh-resolution mass spectrometry. The abundance of CHON compounds (mainly oxygen-poor unsaturated aliphatic-like species) in the positive ion mode was higher in the warm period than in the cold period, which was largely attributed to the contribution of fresh biomass material combustion (e.g., forest fires) associated with amidation of unsaturated fatty acids in the warm period, rather than the oxidation processes. However, CHON compounds (mainly nitro-aromatic species) in the negative ion mode increased significantly in the cold period, which was tightly related to old-age biomass combustion (e.g., dry straws) in wintertime Urumqi. For CHN compounds, alkyl nitriles and aromatic species showed higher abundance in the warm and cold periods, respectively. Alkyl nitriles can be derived from fresh biomass material combustion associated with the dehydration of amides (the main CHON compounds in the warm period). In contrast, aromatic species were tightly related to old-age biomass burning. These findings further suggested different impacts of the combustion of fresh- and old-age biomass materials on NOC compositions in different seasons. The overall results shed light on the mechanisms by which fresh and old-age biomass materials release different NOCs during combustion.

Keywords: Aerosols, Organic nitrogen, Molecular composition, Fresh biomass, Old-

47   age biomass

1. Introduction

50   Fine particulate matter ($PM_{2.5}$) is a typical atmospheric pollutant that can affect the

51   global climate system, as well as urban air quality and human health (Seinfeld et al.,

52   2016; Wang et al., 2021a). Organic aerosol (OA) contributes significantly (20–90%) to

53     $PM_{2.5}$ mass concentration in most polluted areas worldwide (Zhang et al., 2007; Han et

54   al., 2023). Up to 77% of molecules in OA include nitrogen-containing functional groups

55   (Ditto et al., 2020; Kenagy et al., 2021), which have been suggested to play important

56   roles in the formation, transformation, acidity, and hygroscopicity of OA (Xu et al.,

57   2020; Wang et al., 2017b; Laskin et al., 2009). Moreover, the further oxidation or

58   nitrification of some nitrogen-containing organic compounds (NOCs) and volatile

59   organic compounds (VOCs) by ozone (O_3), hydroxyl radical (•OH), and nitrogen oxides

60   (NO_x) can lead to an increase in the health hazards of OA (Franze et al., 2005; Bandowe

61   and Meusel, 2017). Nitrated amino acids and nitrated PAHs are two representative

62   hazard NOCs (Franze et al., 2005; Bandowe and Meusel, 2017). Thus, the identification

63   of aerosol NOCs at the molecular level is important for improving our understanding

64   of the precursors, sources, and formation processes of nitrogen-containing OA.

65   Previous observations in urban, rural, marine, and forest areas have suggested that

66   the molecular composition and relative abundance of aerosol NOCs were spatially

67   different (Samy and Hays, 2013; Jiang et al., 2022; Lin et al., 2012; Xu et al., 2023;

68   Zeng et al., 2021; Zhang et al., 2022; Zeng et al., 2020). These differences can be mainly

69   attributed to the diverse sources and formation mechanisms of aerosol NOCs.

70   Commonly reported primary sources include combustion process releases and natural

71   emissions (e.g., soils, plant debris, pollen, and ocean) (Song et al., 2022; Wang et al.,

72   2017b; Cape et al., 2011; Lin et al., 2023). In addition, aerosol NOCs can also be tightly

73   associated with secondary formation processes involving the reactions of reactive

74   nitrogen with VOCs or particle-phase CHO compounds (Bandowe and Meusel, 2017;

75   Zarzana et al., 2012; Laskin et al., 2014). For example, laboratory experiments have

76   found that the oxidation of isoprene and α-/β-pinene in the presence of NO_x can result

77   in the formation of organic nitrates (e.g., methacryloyl peroxynitrate, dihydroxynitrates,

78   and monohydroxynitrates) (Surratt et al., 2010; Rollins et al., 2012; Nguyen et al., 2015).

79   The reduced nitrogen species (e.g., NH_3, NH_4^+, and organic amines) have been

80   demonstrated to contribute to the formation of NOCs through "carbonyl-to-imine"

81   transformations in the laboratory experiments (Zarzana et al., 2012; Laskin et al., 2014).

82   In the field observation studies, NOCs in particulate matter were analyzed at the

83   molecular level to indicate their sources and formation mechanisms (Jiang et al., 2022;

84   Lin et al., 2012; Zhong et al., 2023). Xu et al. (2023) characterized the variations of

85   molecular compositions in urban road $PM_{2.5}$, suggesting that organic nitrates increased

86   largely through the interactions of atmospheric oxidants, reactive gas-phase organics,

87   and aerosol liquid water. Several field studies conducted in Beijing (China) and

88   Guangzhou (China) also suggested that the molecular compositions and formation of

89   NOCs were tightly associated with environmental conditions (Jiang et al., 2022; Lin et

90   al., 2012; Xie et al., 2020). Generally, most studies on aerosol NOCs were performed

91 in economically developed regions, as well as in forest and marine areas (Jiang et al.,

92 2022; Wang et al., 2017a; Ditto et al., 2022b; Altieri et al., 2016; Xu et al., 2020; Liu et

93 al., 2023; Zhang et al., 2022; Zeng et al., 2020).In contrast, few studies have

94 investigated the sources and atmospheric transformation of NOCs in the northwest

95 border urban of China (e.g., Urumqi) with fragile ecology and harsh environmental

96 conditions (e.g., cold winter and dry summer), which may hinder our comprehensive

97 and in-depth understanding of the formation process of NOCs in ambient aerosols.

98   Biomass burning emissions were widely reported in the source identification of

99 aerosol NOCs in northern and southwestern China because of heating and cooking

100 needs (Zhong et al., 2023; Wang et al., 2021c; Chen et al., 2017). A recent observation

101 study in urban Tianjin suggested that most CHON compounds in wintertime $PM_{2.5}$

102 originated from biomass burning (Zhong et al., 2023). The CHN_2 compounds have been

103 identified in biomass burning OA (BBOA) (Laskin et al., 2009; Wang et al., 2017b).

104 Moreover, the high temperature generated by biomass burning can facilitate the release

105 of ammonia, a process that caused the reaction of carboxylic acids (e.g., oleic acid) with

106 ammonia to form amides and alkyl nitriles (Radzi Bin Abas et al., 2004; Simoneit et al.,

107 2003). Interestingly, we found that biomass burning in rural China typically includes

108 fresh biomass materials (e.g., forest fires) and old-age biomass materials (e.g., straw

109 after autumn harvest, fallen leaf, and deadwood). Fresh biomass is rich in oils and

110 proteins, whereas old-age biomass materials are usually oligotrophic due to the transfer

111 of nutrients to tender tissues or fruits (Jian et al., 2016; Xu and Xiao, 2017). Thus, NOCs

112 released from different types of biomass combustion may vary in molecular

113 compositions. However, there are large gaps in our current knowledge about the

114 impacts of fresh and old-age biomass burning on NOCs in ambient aerosols.

115   Urumqi (northwest China) is the largest inland city farthest from the ocean in the

116 world, which is becoming increasingly prominent due to the national strategy of the

117 "One Belt, One Road." The city and neighboring countries have a dry summer that can

118 easily trigger forest fires (Bátori et al., 2018; Xu et al., 2021), while the winter is

119 freezing with intensive old-age biomass and fuel combustion for heating (Ren et al.,

120 2017). In this study, we presented one-year ambient measurements of the chemical

121 compositions in PM$_{2.5}$ collected from Urumqi. The specific aims of this study are (1) to

122 investigate the molecular-level speciation of functionalized organic nitrogen

123 compounds via high-resolution mass spectrometry with positive (ESI+) and negative

124 (ESI−) ionizations and (2) to investigate the potential sources and formation processes

125 for NOCs with a special focus on the relative influences of fresh and old-age biomass

126 burning in different seasons.

127

128 **2. Materials and methods**

129 **2.1. Study site description and sample collection**

130   The study was conducted in Urumqi city, which has an average altitude of 800 m.

131 The region has an arid temperate continental climate with an annual mean temperature

132 of 7.4 ± 13.9 °C and an annual mean rainfall of 27.8 mm. The sampling site is located

133 in the suburban area (Boda campus of Xinjiang University) of the city (87.75°E,

134 43.86°N) (**Figure S1**), which is characterized by low population and traffic density.

135   This is because Urumqi is relatively vast and sparsely populated compared to developed

136   coastal cities in China (Qizhi et al., 2016). Additionally, the area is surrounded by

137   mountains on three sides, resulting in the difficulty in diffusing air pollutants. The

138   dominant forest trees in this area are *Picea schrenkiana*, *Betula tianschanica* Rupr.,

139   *Populus talassica* Kom., and *Ulmus pumila* L.. The dry climate and strong sunlight in

140   the warm period (18.81 ± 6.4°C, **Table S1**) would be the main culprits of forest fires in

141   the local and nearby areas. In the cold period (−1.96 ± 11.26°C) (**Table S1**), the

142   centralized heating and old-age biomass burning may be the main contributors to local

143   air pollution. Thus, it provides an unexpected opportunity to investigate the potentially

144   differential impacts of fresh and old-age biomass burning on aerosol NOCs.

145   A high-volume air sampler (Series 2031, Laoying, China) was set up on the

146   rooftop of a building (School of Geology and Mining Engineering, Xinjiang University).

147   PM$_{2.5}$ samples (n = 73) were collected every five days with a duration of ~24 h onto

148   prebaked (450 °C for ~ 10 h) quartz fiber filters (Pallflex, Pall Corporation, USA) from

149   1 March 2018 to 26 February 2019. One blank filter was collected every month (n =

150   12). All filter samples were stored at −30°C until further analysis. During the sampling

151   campaigns, the meteorological data (e.g., temperature and relative humidity) and the

152   concentrations of O$_3$ and NO$_x$ were recorded hourly from the adjacent environmental

153   monitoring station. These hourly data were then averaged to obtain daily values to

154   match the sampling time of PM$_{2.5}$. In addition, the trajectories (72 h) of air masses

155   arriving at the sampling site at each sampling event were calculated to investigate the

156   potential influence of pollutant transport on aerosol NOCs.

157

2.2. Chemical analysis

A portion of each filter sample was extracted twice using 3 mL methanol (LC-MS

grade, CNW Technologies Ltd.) under sonication in a chilled ice slurry (~4 °C). The

extracted solutions were filtered through a polytetrafluoroethylene syringe filter (0.22

μm, CNW Technologies GmbH). Subsequently, the extracts were concentrated to 300

μL with a gentle stream of gaseous nitrogen (Shanghai Likang Gas Co., Ltd). The final

extracts were analyzed using an ultra-performance liquid chromatography quadrupole

time-of-flight mass spectrometry equipped with an electrospray ionization (ESI) source

(UPLC-ESI-QToFMS, Waters Acquity Xevo G2-XS) in both ESI+ and ESI− modes

(Wang et al., 2021b). It should be pointed out that UPLC-ESI-MS (i.e., TOF-only) was

used to identify molecular formulas of organic matter, while the functional groups of

the target molecule formulas were deciphered by UPLC-ESI-MS/MS (i.e., tandem mass

spectrometry). Ions obtained from m/z 50–700 were assigned molecule formulas by

assuming hydrogen or sodium adducts in ESI+ mode and deprotonation in ESI− mode.

Detailed chromatographic conditions, parameter selection, and quality control were

displayed in the Supplement (**Sect. S1**). Notably, there may be differences in ionization

efficiencies between compound types. However, the exact impacts of ionization

efficiency on multifunctional compounds in a complex mixture are uncertain and

difficult to evaluate (Ditto et al., 2022b; Yang et al., 2023). Thus, the intercomparison

across compound relative abundance without considering potentially differentiated

ionization efficiency was conducted in this study, which was similar to many previous

179 studies (Xu et al., 2023; Jiang et al., 2022).

180   For the measurement of inorganic ions, a portion of each filter sample was

181 ultrasonically extracted with Milli-Q water (18 MΩ cm) (3 mL) in an ice-water bath

182 (~4 °C). The extract solutions were then filtered via a polytetrafluoroethylene syringe

183 filter (0.22 μm, Millipore, Billerica, MA). The concentrations of water-soluble

184 inorganic ions, including NO_3^-, SO_4^{2-}, Cl^-, Ca^{2+}, Mg^{2+}, Na^+, and NH_4^+ in the samples

185 were determined using an ion chromatograph system (Dionex Aquion, Thermo

186 Scientific, USA) (Xu et al., 2022a; Lin et al., 2023).

187

188 **2.3. Compound categorization and predictions of ALW, pH, and hydroxyl radical**

189   The molecular formulas identified by UPLC-ESI-QToFMS were classified into

190 several major compound classes based on their elemental compositions (i.e., C, H, O,

191 and N), primarily including CHO, CHON, and CHN groups in the ESI+ mode and CHO,

192 CHON, CHOS and CHONS groups in the ESI– mode (Wang et al., 2017b). CHOS and

193 CHONS compounds were also detected in the ESI– mode, with numbers of 398 and

194 112, respectively (**Table S2**). As this study focused mainly on NOCs, sulfur-containing

195 species were not discussed. Unless stated otherwise, all of the detected molecules were

196 reported as neutral molecules. The double-bond equivalent (DBE) and carbon oxidation

197 state (OS_C) were calculated to reflect the unsaturation degree of the organics and the

198 composition evolution of organics that underwent oxidation processes, respectively

199 (details in **Sect. S2**) (Kroll et al., 2011; Xu et al., 2023). The identified compounds can

200 be further classified into four subgroups based on the number of carbon atoms and OS_C

value (Kroll et al., 2011; Xu et al., 2023). Briefly, semi-volatile oxidized organic aerosol (SV-OOA) and low-volatility oxidized organic aerosol (LV-OOA) were associated with multi-step oxidation reactions, with OS_C values between -1 and $+1$ and molecular formulas less than 13 carbon atoms. BBOA has OS_C values ranging from -0.5 to -1.5 and more than seven carbon atmos. Compounds with OS_C values less than -1 and carbon atoms above 20 may be related to hydrocarbon-like organic aerosol (HOA). Additionally, the modified aromaticity index (AI_{mod}) was also calculated to indicate the aromaticity of organic compounds (details in **Sect. S2**) (Koch and Dittmar, 2006). The van Krevelen diagrams and AI_{mod} values have been proposed to further classify organic matter categories (Xu et al., 2023; Su et al., 2021), according to which the identified five subgroups included saturated-like molecules (Sa, $H/C \geq 2.0$), unsaturated aliphatic-like molecules (UA, $1.5 \leq H/C < 2.0$), highly unsaturated-like molecules (HU, $AI_{mod} \leq 0.5$ and $H/C < 1.5$), highly aromatic-like molecules (HA, $0.5 < AI_{mod} \leq 0.66$), and polycyclic aromatic-like molecules (PA, $AI_{mod} > 0.66$). Furthermore, it has been suggested that the above subgroups can be subdivided into O-poor and O-rich compounds depending on their O/C ratio (**Table S8**) (Merder et al., 2020; Zhong et al., 2023).

A thermodynamic model (ISORROPIA-II) was applied to predict the mass concentration of aerosol liquid water (ALW) and the value of pH with particle-phase ion concentrations as well as ambient temperature and relative humidity as the inputs, as detailed in our previous publications (Xu et al., 2020; Xu et al., 2023; Xu et al., 2022b). The model output results based on our data set showed that 94% and 90% of

223 NO_3^- were in the aerosol phase in the cold and warm periods, respectively. Hence, the

224 predictions of pH and ALW were conducted without considering gaseous nitric acid

225 (Guo et al., 2015; Wang et al., 2021c). 78% and 21% of NH_4^+ were in the aerosol phase

226 in the cold and warm periods, respectively. Moreover, it is important to note that

227 gaseous NH_3 measurements were not conducted and ammonia partitioning was not

228 considered in this study. Thus, a bias correction of 1 pH unit was applied to calculate

229 the aerosol pH values (Guo et al., 2015; Wang et al., 2021c). The concentrations of

230 ambient •OH were predicted using empirical formula (Ehhalt and Rohrer, 2000; Wang

231 et al., 2020).

232

233 **3. Results and discussion**

234 **3.1. Overall molecular characterization of organic aerosols**

235 **Figures 1a** and **1c** show the mass spectra of organic compounds detected in ESI+

236 and ESI−, respectively. More compounds were identified in ESI+ (1885 molecular

237 formulas) than in ESI− (1091 molecular formulas) (**Table S2**), which was similar to

238 previous reports about the molecular characteristic of biomass burning aerosols and

239 urban aerosols (Jiang et al., 2022; Wang et al., 2017b). The molecular weights of the

240 compounds with relatively high signal intensity mainly ranged from 100 Da to 500 Da

241 in ESI+, which was larger than those (100–300 Da) observed in the urban (Changchun,

242 Guangzhou, and Shanghai) (Wang et al., 2021a) and agriculture (Suixi) (Wang et al.,

243 2017b) regions of China. In contrast, the species with the strong signal intensity fell

244 between 100 Da and 300 Da in ESI−. This mass range detected in Urumqi organic

245 aerosols was comparable to previous observations in urban (Xi'an) aerosols (Han et

246 al., 2023) but significantly lower than that in firework-related urban (Beijing) aerosols

247 (300–400 Da) (Xie et al., 2020). On average, the molecular number and relative

248 abundance of CHON compounds (150–500 Da) were dominant in ESI+, accounting

249 for 45.57% of the total molecular number and 62.70 ± 6.83% of the total signal

250 intensity (**Figures 1a** and **Table S2**). CHO compounds were the second most abundant

251 categories (28.76 ± 4.75% of the total signal intensity), followed by CHN compounds.

252 However, previous observations conducted in Shanghai, Guangzhou, and Changchun

253 suggested that the compounds in ESI+ were dominated by CHN and CHON species

254 (Wang et al., 2021a). In ESI−, although the number of CHON compounds was less

255 than CHO, the relative abundance of CHON compounds (150–250 Da) was higher

256 (**Figures 1d** and **Table S2**). The finding was consistent with the results obtained in

257 Shanghai and Changchun but different from the case in Guangzhou (Wang et al.,

258 2021a). The average H/C ratios of CHO (1.62−1.66) and CHON (1.79−1.83)

259 compounds in ESI+ mode (**Table S3**) were higher than those (0.94−1.13 for CHO and

260 1.27−1.47 for CHON) in Changchun, Shanghai, and Guangzhou (Wang et al., 2021a).

261 However, the average O/C ratios of CHO (0.25−0.3) and CHON (0.22−0.3)

262 compounds in ESI+ mode (**Table S3**) were less than those (0.42−0.43 for CHO and

263 0.27−0.45 for CHON) in the urban areas (Shanghai and Guangzhou) (Wang et al.,

264 2021a). Overall, these dissimilarities in molecular characteristics of organic aerosols

265 between Urumqi and other areas may be attributed to their different sources and

266 formation mechanisms.

267   **Figures 1b** and **1d** show the time series of the fractional distributions of various

268   organic matter categories in different ion modes. The abundance of CHO compounds

269   in ESI+ exhibited a temporal variation similar to that of CHON compounds ($r = 0.51$,

270     $P < 0.01$), with increased levels in the warm period. This indicated that CHO

271   compounds may be important precursors for the formation of NOCs (via reactions in

272   the gas- and/or particle-phases) or that they have similar origins. Previous simulation

273   experiments have demonstrated that higher temperatures increase the concentration of

274   oxygenated organic molecules, while lower temperatures can allow less oxidized

275   species to condense (Stolzenburg et al., 2018; Frege et al., 2018). In addition, solar

276   radiation and atmospheric oxidation capacity are also important factors promoting the

277   formation of more oxygenated organic molecules (Li et al., 2022; Liu et al., 2022). Air

278   temperature, radiation, and atmospheric oxidation capacity were much higher in the

279   warm period than in the cold period in Urumqi (**Table S1**) (Wan et al., 2021), which

280   may be partly responsible for increased abundances of CHO and CHON compounds in

281   the warm period. However, the abundance of CHN compounds tended to increase from

282   the warm period to the cold period. Since the ESI+ mode is highly sensitive to

283   protonatable species, organic amines were expected to predominate the CHN

284   compounds (Han et al., 2023; Wang et al., 2021a). It is well documented that the

285   formation of amine salt in the particle phase is tightly associated with aerosol acidity

286   and water (Liu et al., 2023). Thus, the reduced pH value and increased ALW level in

287   the cold period (**Table S1**) provided greater potential for converting gaseous amines

288   into particles.

In ESI− mode, the abundances of CHON and CHO compounds exhibited a significantly increased level in the cold period (**Figure 1d**), a variation pattern which was completely opposite to the case in ESI+ mode. The ESI− mode is more sensitive to deprotonatable compounds like nitrophenols, organic nitrates, organosulfates, and organic acids (Jiang et al., 2022; Lin et al., 2012). The formations of these compounds were highly impacted by ALW and aerosol acidity (Ma et al., 2021; Smith et al., 2014; Zhou et al., 2023; Xu et al., 2023). However, Urumqi has dry and dusty weather, particularly in warm period, resulting in a quite low ALW concentration (1.86 ± 1.90 $\mu g\ m^{-3}$) in the warm period (**Table S1**). Moreover, the calculated mean pH value was 6.86 ± 1.71 (**Table S1**) during the warm period, which implies that the fine aerosol particles in the warm period in Urumqi was neutral or slightly alkaline. Obviously, the aerosol characteristics of the warm period in Urumqi may hinder the formation of these organic compounds measured in ESI− mode. In contrast, the increased ALW concentration and decreased pH value during the cold period can facilitate the formation of CHO and CHON compounds through the partitioning of gas-phase species to the particles and subsequent aqueous phase reactions (Xu et al., 2020; Xu et al., 2023). Furthermore, the total signal intensity of CHO compounds was significantly correlated with that of CHON ($r = 0.62$, $P < 0.01$), indicating that they may have similar origins or that CHO compounds may serve as important precursors for CHON compound formation. In general, the differentiated seasonal variation patterns for the different types of NOCs measured here can be attributed to the unique meteorological conditions in Urumqi and different ionization mechanisms in ESI+ and ESI− modes. The sources

311   and formation mechanisms of NOCs will be further discussed in the following sections.

312

313   **3.2. Seasonally differential sources and formation mechanisms of CHON**

314   **compounds**

315   CHON compounds can be derived from the reactions between CHO species and

316   reactive nitrogen species (NO_x, NH_3, and NH_4^+) (Lee et al., 2016; De Haan et al., 2017),

317   as also partly implied by significant positive correlations (r = 0.51–0.62, P < 0.01)

318   between total signal intensity of CHO and CHON compounds in both ESI+ and ESI−

319   modes. Thus, CHO compounds were further classified based on their OS_C values to

320   preliminarily explore their origins and linkages with CHON compound formation

321   (**Figures 2a** and **2b**). In ESI+ mode, the OS_C values of the detected CHO compounds

322   (−1.75 to 0.5) were higher than those of primary vehicle exhausts (−2.0 to −1.9) (Aiken

323   et al., 2008), likely indicating a weak (or indirect) contribution of primary vehicle

324   exhausts to CHO molecules in Urumqi. The signal intensity of BBOA dominated the

325   total OA signal intensity and was higher in the warm period than in the cold period

326   (**Figure 2e**). However, previous studies conducted in China (e.g., Beijing, Xi'an,

327   Shanghai, and Liaocheng) suggested that biomass burning was more significant in the

328   cold seasons (Li et al., 2023; Wang et al., 2017a; Chen et al., 2017; Wang et al., 2009;

329   Wang et al., 2018; Zhang et al., 2022). Furthermore, we found that the oxygen-poor

330   unsaturated aliphatic compounds showed a high signal intensity in the warm period and

331   that the signal intensities of all categories of compounds in the warm period were

332   weakly correlated with atmospheric oxidants (i.e., O_3 and •OH) (r < 0.1, P > 0.05).

Thus, the formation or source of CHO compounds in the warm period may not be mainly controlled by high atmospheric oxidation but rather by biomass burning, which was distinguished from previous reports (Duan et al., 2020; Kondo et al., 2007; Zhang et al., 2023). This consideration was also supported by the fact that there were significantly more fire spots in the warm period than in the cold period (**Figure 3**). It should be noted that the materials used for biomass burning in the cold period in rural China are typically old-age plant tissues, such as dead branches of pine trees, dead branches of shrubs, corn straw, and rice straw (**Figure S3**), while biomass burning in the warm season is mainly attributed to forest fires or wildfires (relatively fresh biomass). Accordingly, a large number of fresh biomass material burning occurred from April to October each year in the neighboring countries (e.g., Kazakhstan) (Xu et al., 2021) or regions of Urumqi (due to drought) (**Figure 3**) may be largely responsible for high CHO compound abundance in the warm period.

The CHO species in ESI$-$ had higher OS_C (-1.85 to 1.1) than those in ESI$+$ (-1.85 to 0.25) (**Figures 2c** and **2d**), which was consistent with a recent study conducted in Guangzhou, China (Zou et al., 2023). The predominant subgroups of CHO in ESI$-$ were BBOA (66.4% of total signal intensity) and SV-OOA (23.1% of total signal intensity), which was different from the observation in Shanghai (dominated by SV-OOA and LV-OOA) (Wang et al., 2017a). Additionally, some specific saturated and unsaturated aliphatic CHO substances (i.e., $C_{12-18}H_nO_2$) in ESI$-$ showed higher abundance in the warm season than in the cold season, which was contrary to the variation pattern of other CHO compounds. These $C_{12-18}H_nO_2$ compounds were found

355 to be mainly fatty acids, such as stearic acid ($C_{18}H_{36}O_2$), oleic acid ($C_{18}H_{34}O_2$),

356 linolelaidic acid ($C_{18}H_{32}O_2$), palmitic acid ($C_{16}H_{32}O_2$), and palmitoleic acid ($C_{16}H_{30}O_2$)

357 (**Figure S4**), all of which usually accumulate in plants, particularly *Suaeda*

358 *aralocaspica* (W. Hogg and T. Gillan, 1984; Wang et al., 2011). Interestingly, this plant

359 was widely distributed in Central Asia as well as on the southern edge of the Junggar

360 Basin in Xinjiang, China (Wang et al., 2011). Although fatty acids can also originate

361 from food cooking (Zhao et al., 2007), there seem to be no seasonal differences in

362 cooking behavior locally. Thus, these results further confirmed our consideration that

363 the abundance of CHO compounds in the warm period was highly impacted by fresh

364 biomass material burning (e.g., forest fires or wildfires).

365   CHON molecules in ESI+ were mainly identified as unsaturated aliphatic-like

366 compounds that are oxygen poor (**Figures 4a** and **4b**), accounting for more than 70%

367 of the total signal intensities of CHON species (**Figure S5**). The signal intensity of

368 CHON species in ESI+ was greater in the warm period than in the cold period (**Figure**

369 **4e**). Moreover, BBOA contributed to 56.9 % of the total CHON signal intensity in the

370 warm period (**Figure S6**). These characteristics of CHON compounds were similar to

371 those of CHO. Considering a significant positive correlation ($r = 0.62$, $P < 0.01$)

372 between the total signal intensity of CHO and CHON compounds in ESI+, we thus

373 concluded that primary sources (i.e., fresh biomass material burning) were also one of

374 the main sources of CHON compounds. In this study, CHON compounds with O/N <

375 3 contributed 76.48 ± 1.11% of total CHON species in ESI+ (**Figure S7**), which was

376 much larger than the results observed in urban Tianjin in winter (less than 20%) (Zhong

377 et al., 2023). In particular, $C_{16}H_{33}ON$, $C_{18}H_{37}ON$, $C_{18}H_{35}ON$, $C_{18}H_{33}ON$, $C_{18}H_{31}ON$,

378 and $C_{20}H_{33}ON$ showed a high abundance, together accounting for 55.04 ± 7.09 % of

379 the total CHON abundance (**Table S4**). The carbon number of these compounds was

380 consistent with that of fatty acids mentioned above; moreover, their abundances showed

381 a positive correlation (r = 0.43–0.81, P < 0.01) with the abundances of corresponding

382 fatty acids in the warm period. In contrast, these CHON compounds only showed a

383 weak correlation (r = −0.24 ∼ 0.33) with atmospheric oxidants (e.g., •OH, O_3, and NO_x).

384 Thus, the formation mechanism of biomass burning-related NOCs in Urumqi during

385 the warm period may be the interaction between fatty acids and reduced nitrogen

386 species (e.g., NH_3) rather than the oxidation pathway involving CHO compounds and

387 NO_x.

388   A recent laboratory study has suggested that NH_3 produced during the thermal

389 degradation of amino acids can react with oleic acid from the pyrolysis of triglycerides

390 to form amides (R1) (Ditto et al., 2022a). As discussed above, the combustion of fresh

391 biomass materials (e.g., forest fires or wildfires) can release abundant fatty acids. In

392 addition, wildfires can also emit large amounts of NH_3, with an average emission factor

393 more than twice the NH_3 emission factor of agricultural fires (Tomsche et al., 2023).

394 According to MS/MS analysis (**Table S5**), potential fatty acid-derived NOCs were

395 indeed identified as amides. Thus, we proposed that the high temperature generated

396 during wildfires or forest fires provides suitable conditions for the reaction of

397 carboxylic acids and NH_3 to form amides. The specific process was presented in **Figure**

398 **5** (Pathway 1). It has been suggested that atmospheric oxidants can oxidize olefins (R2

399 and R3) to form hydroxyl nitrates and carbonyl nitrates (Perring et al., 2013). Therefore,

400 fatty acids (oleic acid as a representative) released from fresh biomass material burning

401 may also rely on oxidation pathways to form NOCs (**Figure 5**, Pathway 2). It is worth

402 noting that some products with double bonds after the amidation of unsaturated fatty

403 acids can continue to undergo the reactions of R2 and R3 in the atmosphere, resulting

404 in the formation of nitrooxy amides (**Figure 5**, Pathway 3). However, we found that the

405 abundance of oleic acid-derived amides via Pathway 1 in the warm period was more

406 than 100 times higher than that of NOCs with $-ONH_2$ (thus, the impact of ionization

407 efficiency is expected to be less than 100 times) from Pathways 3. In the cold period,

408 the abundance of fatty acids-derived amides decreased dramatically (**Figure 5** and

409 **Figure S8**). Thus, the overall results demonstrated that the combustion of fresh biomass

410 materials indeed contributed significantly to aerosol NOCs (e.g., amides) in the warm

411 period in Urumqi.

412 $$ROOH \xrightarrow[-H_2O \text{ and high temperature}]{NH_3} RCONH_2 \tag{R1}$$

413 $$RH \xrightarrow{\cdot OH} R\cdot \xrightarrow{O_2} RO_2\cdot \xrightarrow{NO} RONO_2 \tag{R2}$$

414 $$R_1=R_2 \xrightarrow{NO_3\cdot} R_1(ONO_2)\text{-}R_2\cdot \xrightarrow{O_2} R_1(ONO_2)\text{-}R_2O_2\cdot \xrightarrow{RO_2\cdot,\ NO_3\cdot} R_1(ONO_2)\text{-}R_2(O) \tag{R3}$$
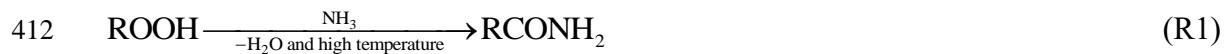
415 The CHON species detected in ESI− were mainly aromatic-like compounds,

416 whose signal intensities were significantly greater in the cold period than in the warm

417 period (**Figures 4c,4e** and **Figure S5**). Moreover, we found that several nitro-aromatic

418 compounds, including $C_6H_5O_3N$, $C_6H_5O_4N$, $C_7H_7O_3N$, $C_7H_7O_4N$, $C_7H_5O_5N$, and

419 $C_8H_9O_3N$ (confirmed by their authentic standards in the LC/MS analysis), contributed

up to 50% of the total CHON (ESI− mode) intensity (**Table S6**). Other NOCs with relatively high signal intensity were mainly $O_{4-6}N_2$ species (contributed up to 25%), such as $C_6H_4O_5N_2$, $C_7H_4O_7N_2$, $C_7H_6O_5N_2$, and $C_7H_6O_6N_2$, which have been suggested to be associated with secondary photochemical or multiphase chemical processes (Harrison et al., 2005; Cecinato et al., 2005; Salvador et al., 2021). However, the abovementioned nitro-aromatic compounds including $C_6H_5O_3N$ (nitrophenol), $C_6H_5O_4N$ (nitrocatechol), $C_7H_7O_3N$ (methyl-nitrophenol), and $C_7H_7O_4N$ (methyl-nitrocatechol) were primarily identified as tracers of straw and wood burning (old-age biomass materials commonly used in suburban and rural China) (Iinuma et al., 2010; Kourtchev et al., 2016). A study about molecular characterization (ESI− mode) of water-soluble aerosols emitted from the combustion of old-age biomass materials (i.e., dry corn straw, rice straw, and pine branches) and coal showed that OA from old-age biomass burning typically contained much more nitro compounds and/or organonitrates than that from coal, while OA from coal-smoke contained more sulfur-containing compounds (Song et al., 2018). Thus, the old-age biomass burning associated with winter heating rather than coal combustion may contribute a significant amount of aerosol NOCs (e.g., nitrophenols) in wintertime Urumqi. However, it does not necessarily suggest that the importance of multiphase chemistry in the formation of NOCs was ignorable, as indicated by relatively high signal intensity of $O_{4-6}N_2$ species. In general, the differential molecular characteristics of CHON species in different seasons in Urumqi can largely attributed to different impacts of the combustion of fresh- and old-age biomass materials.

442

3.3. CHN molecule evidence of fresh and old-age biomass burning in different periods.

Figures 6a and **6b** present the van Krevelen diagram of CHN compounds in the cold and warm periods. The CHN_1 compounds with relatively high signal intensity mainly contained 7–20 carbon atoms, among which $C_5H_5N(CH_2)_n$, $C_9H_7N(CH_2)_n$, and $C_{13}H_9N(CH_2)_n$ were dominant (78.68 ± 7.59 % of the total signal intensity of CHN_1 compounds in the cold period, **Table S7**). $C_5H_5N(CH_2)_n$ could be identified as pyridine and its homologues, which have been detected in freshly discharged BBOA (Dou et al., 2015). Additionally, the abundance of $C_5H_5N(CH_2)_n$ was positively correlated with that of $C_9H_7N(CH_2)_n$, $C_{13}H_9N(CH_2)_n$, and nitro-aromatic compounds mentioned above ($r = 0.46-0.81$, $P < 0.01$), particularly in the cold period with old-age biomass burning for heating. We further found that both the total signal intensity and aromaticity of CHN_1 species were much higher in the cold period (AI_{mod} of 0.52) than in the warm period (AI_{mod} of 0.35) (**Figure 6** and **Figure S9**). It has been suggested that old-age leaves contain more aromatic compounds compared to fresh leaves (Jian et al., 2016). Thus, the overall results implied that old-age biomass burning had an important contribution to the variation of CHN_1 compounds. In particular, the intensity of CHN_1 compounds was significantly negatively correlated with the concentration of O_3 and $\cdot OH$ ($r = -0.44 \sim -0.53$, $P < 0.01$), suggesting that atmospheric oxidation processes were the potential pathway for amine removal rather than the sources of particle amine salts (Zahardis et al., 2008; Qiu and Zhang, 2013). This result differed from the previous case, which

464   showed that the formation processes of CHN_1 and its homologs in Guangzhou (South

465   China) were tightly related to photo-oxidation processes (Jiang et al., 2022). The CHN_2

466   species showed a similar temporal variation pattern to the CHN_1 species. Moreover, the

467   abundances of total CHN_2 and major components ($C_{8-11}H_8N_2(CH_2)_n$, $C_{10}H_{14}N_2(CH_2)_n$,

468     $C_{10}H_{16}N_2(CH_2)_n$ and $C_5H_8N_2(CH_2)_n$) were positively correlated with that of total CHN_1

469   ($r = 0.55-0.90$, $P < 0.01$), but negatively correlated with the concentration of O_3

470   and $\cdot OH$ ($r = -0.43 \sim -0.60$, $P < 0.01$). Clearly, old-age biomass burning, particularly

471   in the cold period, also exerted significant impacts on the abundance of CHN_2

472   compounds, which was also supported by several previous studies (Laskin et al., 2009;

473   Wang et al., 2017b; Song et al., 2022). A study about molecular characterization (ESI+

474   mode) of humic-like substances emitted from the combustion of old-age biomass

475   materials (i.e., dry corn straw, rice straw, and pine branches) and coals showed that OA

476   from old-age biomass burning typically contained much more CHN_2 compounds (55–

477   64%) than that from coal (20–37%), while OA from coal-smoke showed more CHN_1

478   compounds (78–84%) compared to that from old-age biomass materials (15–22%)

479   (Song et al., 2022). In this study, the signal intensity of CHN_1 compounds in the cold

480   period was about 40% higher than that in the warm period, while that of CHN_2

481   compounds showed a 160% increase from the warm period to the cold period. Thus,

482   although the contribution of fossil fuel (e.g., coal) combustion to NOCs in the cold

483   period cannot be ignored, our results at least suggested that the biomass burning-derived

484   CHN compounds showed a more significant increase compared to coal combustion-

485   derived compounds from the warm period to the cold period in Urumqi.

Interestingly, we found some CHN species with 16–20 carbon atoms showed

higher abundance in the warm period than in the cold period, a pattern opposite to that

of all other CNH compounds (**Figure 6c**). These $C_{16-20}N_1H_x$ compounds were further

identified as alkyl nitriles (**Table S5**) (Simoneit et al., 2003). In addition, the carbon

number of the identified alkyl nitriles was consistent with those of amides previously

proposed to be produced by fresh biomass burning. Thus, we proposed that fresh

biomass material burning in the warm period may provide a continuous high-

temperature environment to promote the dehydration of amides (**Figure 5**, Pathway 4).

These alkyl nitriles with double bonds can continue to undergo the reactions of R2 and

R3 **(Figure 5**, Pathway 5)**. However, the signal intensity of the nitrooxy products in the

warm period was insignificantly correlated with the concentration of O_3, $\cdot OH$, and NO_x

($P > 0.05$), likely indicating a weak influence of atmospheric oxidation on alkyl nitrile

removal in this site. The high-temperature dehydration of amides (e.g., erucamide) to

form alkyl nitriles (e.g., erucyl nitrile) has been demonstrated by Simoneit et al. (2003)

in a laboratory simulation experiment. A study on BBOA also showed that alkyl nitriles

can be serve as indicators of biomass burning in the ambient atmosphere (Radzi Bin

Abas et al., 2004). Furthermore, the abundance of identified alkyl nitriles initially

increased from March and peaked in September and October (**Figure S10**), a pattern

which was consistent with the interannual variation in wildfire areas (more in the warm

period) in Central Asian countries (Xu et al., 2021). Although cooking is also a potential

source of alkyl nitriles (Schauer et al., 1999), this activity does not have seasonal

differences. In contrast, the dramatically increased abundance of aromatic CNH

508   compounds in the cold period (**Figure S9**) can be attributed to the aqueous reactions of

509   amines emitted from old-age biomass material and coal combustion with acidic

510   substances, as indicated by significant correlations ($r = 0.61-0.95$, $P < 0.01$) between

511   total CHN abundance and SO_4^{2-} and NO_3^- concentrations. These findings further

512   confirmed that the NOCs from the combustion of fresh biomass materials in the warm

513   period in suburban Urumqi were compositionally different from those from old-age

514   biomass burning in the cold period.

515

516   **4. Conclusions**

517   The complexity of NOCs restricts our understanding of its sources and formation

518   processes. In this study, the molecular compositions of organic aerosols in $PM_{2.5}$

519   collected in Urumqi over a one-year period were systematically characterized in both

520   ESI− and ESI+ modes, with a major focus on NOCs. A large amount of NOCs were

521   identified, showing that NOCs in relatively highly oxidative and reduced forms can be

522   roughly distinguished via these two ionization modes. Based on the identification of

523   molecular markers of amides and alkyl nitriles (much higher in the warm period) and

524   the analysis of their formation mechanisms (less contribution of atmospheric oxidation),

525   we highlighted the important contribution of combustion of fresh biomass materials

526   such as forest fires and wildfires to NOCs in the warm season in Urumqi. In contrast,

527   the dramatically increased abundances of aromatic CNH compounds and nitro-aromatic

528   CHON compounds (mainly nitrophenols) in the cold period were tightly associated

529   with the impacts of old-age biomass material burning. These results were illustrated in

530 a diagram (**Figure 7**).

531   Biomass materials in rural China were typically old-age plant tissues, as

532 mentioned above. Fresh biomass materials (e.g., green vegetation) with the enrichment

533 of oils and proteins can exist in forest fires or wildfires. Indeed, previous studies have

534 suggested that biomass burning can lead to the formation of aerosol amines and nitriles.

535 However, field observation studies have yet to pay attention to the differences in aerosol

536 NOCs emitted from the combustion of fresh and old-age biomass materials. For the

537 first time, our results reveal that fresh biomass material combustion can contribute more

538 amines and nitriles than old-age biomass material combustion. Generally, this study

539 provides field evidence on the differential impacts of the combustion of fresh and old-

540 age biomass materials on aerosol NOCs, improving our current understanding of the

541 molecular compositions of organic nitrogen aerosols in a vast territory with a sparse

542 population in Northwest China. Moreover, according to the fact that the studied site is

543 highly affected by combustion emissions of different types of biomass materials, future

544 work is needed to deeply understand the quantitative contributions of different types of

545 biomass burning to OA in China.

546

547 **Data availability.** The data in this study are available at

548 https://doi.org/10.5281/zenodo.10453929

549

550 **Competing interests.** The authors declare no conflicts of interest relevant to this study.

551

Supplement. Details of chemical analysis and data processing, eight tables (Tables S1−S8), and ten extensive figures (Figures S1−S10).

Author contributions. YX designed the study. YJM, TY, and HWX performed field measurements and sample collection; YJM and TY performed chemical analysis; YX and YJM performed data analysis; YX and YJM wrote the original manuscript; and YX, YJM, HWX, and HYX reviewed and edited the manuscript.

Financial support. This study was kindly supported by the National Natural Science Foundation of China through grant 42303081 (Y. Xu) and Shanghai "Science and Technology Innovation Action Plan" Shanghai Sailing Program through grant 22YF1418700 (Y. Xu).

References

Aiken, A. C., Decarlo, P. F., Kroll, J. H., Worsnop, D. R., Huffman, J. A., Docherty, K. S., Ulbrich, I. M., Mohr, C., Kimmel, J. R., Sueper, D., Sun, Y., Zhang, Q., Trimborn, A., Northway, M., Ziemann, P. J., Canagaratna, M. R., Onasch, T. B., Alfarra, M. R., Prevot, A. S., Dommen, J., Duplissy, J., Metzger, A., Baltensperger, U., and Jimenez, J. L.: O/C and OM/OC ratios of primary, secondary, and ambient organic aerosols with high-resolution time-of-flight aerosol mass spectrometry, Environ. Sci. Technol., 42, 4478-4485, https://doi.org/10.1021/es703009q, 2008.

Altieri, K. E., Fawcett, S. E., Peters, A. J., Sigman, D. M., and Hastings, M. G.:

Marine biogenic source of atmospheric organic nitrogen in the subtropical North Atlantic, P. Natl. Acad. Sci. USA, 113, 925-930, https://doi.org/10.1073/pnas.1516847113, 2016.

Bandowe, B. A. M. and Meusel, H.: Nitrated polycyclic aromatic hydrocarbons (nitro-PAHs) in the environment – A review, Sci. Total Environ., 581-582, 237-257, https://doi.org/10.1016/j.scitotenv.2016.12.115, 2017.

Bátori, Z., Erdős, L., Kelemen, A., Deák, B., Valkó, O., Gallé, R., Bragina, T. M., Kiss, P. J., Kröel-Dulay, G., and Tölgyesi, C.: Diversity patterns in sandy forest-steppes: a comparative study from the western and central Palaearctic, Biodivers. Conserv., 27, 1011-1030, https://doi.org/10.1007/s10531-017-1477-7, 2018.

Cape, J. N., Cornell, S. E., Jickells, T. D., and Nemitz, E.: Organic nitrogen in the atmosphere — Where does it come from? A review of sources and methods, Atmos. Res., 102, 30-48, https://doi.org/10.1016/j.atmosres.2011.07.009, 2011.

Cecinato, A., Di Palo, V., Pomata, D., Tomasi Scianò, M. C., and Possanzini, M.: Measurement of phase-distributed nitrophenols in Rome ambient air, Chemosphere, 59, 679-683, https://doi.org/10.1016/j.chemosphere.2004.10.045, 2005.

Chen, J., Li, C., Ristovski, Z., Milic, A., Gu, Y., Islam, M. S., Wang, S., Hao, J., Zhang, H., He, C., Guo, H., Fu, H., Miljevic, B., Morawska, L., Thai, P., Lam, Y. F., Pereira, G., Ding, A., Huang, X., and Dumka, U. C.: A review of biomass burning: Emissions and impacts on air quality, health and climate in China, Sci. Total Environ., 579, 1000-1034, https://doi.org/10.1016/j.scitotenv.2016.11.025, 2017.

De Haan, D. O., Hawkins, L. N., Welsh, H. G., Pednekar, R., Casar, J. R.,

596   Pennington, E. A., de Loera, A., Jimenez, N. G., Symons, M. A., Zauscher, M., Pajunoja,

597   A., Caponi, L., Cazaunau, M., Formenti, P., Gratien, A., Pangui, E., and Doussin, J.-F.:

598   Brown Carbon Production in Ammonium- or Amine-Containing Aerosol Particles by

599   Reactive Uptake of Methylglyoxal and Photolytic Cloud Cycling, Environ. Sci.

600   Technol., 51, 7458-7466, https://doi.org/10.1021/acs.est.7b00159, 2017.

601   Ditto, J. C., Abbatt, J. P. D., and Chan, A. W. H.: Gas- and Particle-Phase Amide

602   Emissions from Cooking: Mechanisms and Air Quality Impacts, Environ. Sci. Technol.,

603   56, 7741-7750, https://doi.org/10.1021/acs.est.2c01409, 2022a.

604   Ditto, J. C., Machesky, J., and Gentner, D. R.: Analysis of reduced and oxidized

605   nitrogen-containing organic compounds at a coastal site in summer and winter, Atmos.

606   Chem. Phys., 22, 3045-3065, https://doi.org/10.5194/acp-22-3045-2022, 2022b.

607   Ditto, J. C., Joo, T., Slade, J. H., Shepson, P. B., Ng, N. L., and Gentner, D. R.:

608   Nontargeted Tandem Mass Spectrometry Analysis Reveals Diversity and Variability in

609   Aerosol Functional Groups across Multiple Sites, Seasons, and Times of Day, Environ.

610   Sci. Technol. Lett., 7, 60-69, https://doi.org/10.1021/acs.estlett.9b00702, 2020.

611   Dou, J., Lin, P., Kuang, B.-Y., and Yu, J. Z.: Reactive Oxygen Species Production

612   Mediated by Humic-like Substances in Atmospheric Aerosols: Enhancement Effects by

613   Pyridine, Imidazole, and Their Derivatives, Environ. Sci. Technol., 49, 6457-6465,

614   https://doi.org/10.1021/es5059378, 2015.

615   Duan, J., Huang, R. J., Li, Y., Chen, Q., Zheng, Y., Chen, Y., Lin, C., Ni, H., Wang,

616   M., Ovadnevaite, J., Ceburnis, D., Chen, C., Worsnop, D. R., Hoffmann, T., O'Dowd,

617   C., and Cao, J.: Summertime and wintertime atmospheric processes of secondary

618 aerosol in Beijing, Atmos. Chem. Phys., 20, 3793-3807, https://doi.org/10.5194/acp-

619 20-3793-2020, 2020.

620 Ehhalt, D. H. and Rohrer, F.: Dependence of the OH concentration on solar UV, J.

621 Geophys. Res.-Atmos., 105, 3565-3571, https://doi.org/10.1029/1999JD901070, 2000.

622 Franze, T., Weller, M. G., Niessner, R., and Pöschl, U.: Protein Nitration by

623 Polluted Air, Environ. Sci. Technol., 39, 1673-1678, https://doi.org/10.1021/es0488737,

624 2005.

625 Frege, C., Ortega, I. K., Rissanen, M. P., Praplan, A. P., Steiner, G., Heinritzi, M.,

626 Ahonen, L., Amorim, A., Bernhammer, A. K., Bianchi, F., Brilke, S., Breitenlechner,

627 M., Dada, L., Dias, A., Duplissy, J., Ehrhart, S., El-Haddad, I., Fischer, L., Fuchs, C.,

628 Garmash, O., Gonin, M., Hansel, A., Hoyle, C. R., Jokinen, T., Junninen, H., Kirkby, J.,

629 Kürten, A., Lehtipalo, K., Leiminger, M., Mauldin, R. L., Molteni, U., Nichman, L.,

630 Petäjä, T., Sarnela, N., Schobesberger, S., Simon, M., Sipilä, M., Stolzenburg, D., Tomé,

631 A., Vogel, A. L., Wagner, A. C., Wagner, R., Xiao, M., Yan, C., Ye, P., Curtius, J.,

632 Donahue, N. M., Flagan, R. C., Kulmala, M., Worsnop, D. R., Winkler, P. M., Dommen,

633 J., and Baltensperger, U.: Influence of temperature on the molecular composition of

634 ions and charged clusters during pure biogenic nucleation, Atmos. Chem. Phys., 18, 65-

635 79, https://doi.org/10.5194/acp-18-65-2018, 2018.

636 Guo, H., Xu, L., Bougiatioti, A., Cerully, K. M., Capps, S. L., Hite Jr, J. R., Carlton,

637 A. G., Lee, S. H., Bergin, M. H., Ng, N. L., Nenes, A., and Weber, R. J.: Fine-particle

638 water and pH in the southeastern United States, Atmos. Chem. Phys., 15, 5211-5228,

639 https://doi.org/10.5194/acp-15-5211-2015, 2015.

640   Han, Y., Zhang, X., Li, L., Lin, Y., Zhu, C., Zhang, N., Wang, Q., and Cao, J.:

641   Enhanced Production of Organosulfur Species during a Severe Winter Haze Episode in

642   the Guanzhong Basin of Northwest China, Environ. Sci. Technol.,

643   https://doi.org/10.1021/acs.est.3c02914, 2023.

644   Harrison, M. A. J., Barra, S., Borghesi, D., Vione, D., Arsene, C., and Iulian Olariu,

645   R.: Nitrated phenols in the atmosphere: a review, Atmos. Environ., 39, 231-248,

646   https://doi.org/10.1016/j.atmosenv.2004.09.044, 2005.

647   Iinuma, Y., Böge, O., Gräfe, R., and Herrmann, H.: Methyl-Nitrocatechols:

648   Atmospheric Tracer Compounds for Biomass Burning Secondary Organic Aerosols,

649   Environ. Sci. Technol., 44, 8453-8459, https://doi.org/10.1021/es102938a, 2010.

650   Jian, Q., Boyer, T. H., Yang, X., Xia, B., and Yang, X.: Characteristics and DBP

651   formation of dissolved organic matter from leachates of fresh and aged leaf litter,

652   Chemosphere, 152, 335-344, https://doi.org/10.1016/j.chemosphere.2016.02.107, 2016.

653   Jiang, H., Li, J., Tang, J., Zhao, S., Chen, Y., Tian, C., Zhang, X., Jiang, B., Liao,

654   Y., and Zhang, G.: Factors Influencing the Molecular Compositions and Distributions

655   of Atmospheric Nitrogen-Containing Compounds, J. Geophys. Res.-Atmos., 127,

656   e2021JD036284, https://doi.org/10.1029/2021JD036284, 2022.

657   Kenagy, H. S., Romer Present, P. S., Wooldridge, P. J., Nault, B. A., Campuzano-

658   Jost, P., Day, D. A., Jimenez, J. L., Zare, A., Pye, H. O. T., Yu, J., Song, C. H., Blake,

659   D. R., Woo, J.-H., Kim, Y., and Cohen, R. C.: Contribution of Organic Nitrates to

660   Organic Aerosol over South Korea during KORUS-AQ, Environ. Sci. Technol., 55,

661   16326-16338, https://doi.org/10.1021/acs.est.1c05521, 2021.

662   Koch, B. P. and Dittmar, T.: From mass to structure: an aromaticity index for high-

663   resolution mass data of natural organic matter, Rapid Commun. Mass Spectrom., 20,

664   926-932, https://doi.org/10.1002/rcm.2386, 2006.

665   Kondo, Y., Miyazaki, Y., Takegawa, N., Miyakawa, T., Weber, R. J., Jimenez, J.

666   L., Zhang, Q., and Worsnop, D. R.: Oxygenated and water-soluble organic aerosols in

667   Tokyo, J. Geophys. Res.-Atmos., 112, https://doi.org/10.1029/2006JD007056, 2007.

668   Kourtchev, I., Godoi, R. H. M., Connors, S., Levine, J. G., Archibald, A. T., Godoi,

669   A. F. L., Paralovo, S. L., Barbosa, C. G. G., Souza, R. A. F., Manzi, A. O., Seco, R.,

670   Sjostedt, S., Park, J. H., Guenther, A., Kim, S., Smith, J., Martin, S. T., and Kalberer,

671   M.: Molecular composition of organic aerosols in central Amazonia: an ultra-high-

672   resolution mass spectrometry study, Atmos. Chem. Phys., 16, 11899-11913,

673   https://doi.org/10.5194/acp-16-11899-2016, 2016.

674   Kroll, J. H., Donahue, N. M., Jimenez, J. L., Kessler, S. H., Canagaratna, M. R.,

675   Wilson, K. R., Altieri, K. E., Mazzoleni, L. R., Wozniak, A. S., Bluhm, H., Mysak, E.

676   R., Smith, J. D., Kolb, C. E., and Worsnop, D. R.: Carbon oxidation state as a metric

677   for describing the chemistry of atmospheric organic aerosol, Nat. Chem., 3, 133-139,

678   https://doi.org/10.1038/nchem.948, 2011.

679   Laskin, A., Smith, J. S., and Laskin, J.: Molecular Characterization of Nitrogen-

680   Containing Organic Compounds in Biomass Burning Aerosols Using High-Resolution

681   Mass   Spectrometry,   Environ.   Sci.   Technol.,   43,   3764-3771,

682   https://doi.org/10.1021/es803456n, 2009.

683   Laskin, J., Laskin, A., Nizkorodov, S. A., Roach, P., Eckert, P., Gilles, M. K., Wang,

B., Lee, H. J., and Hu, Q.: Molecular Selectivity of Brown Carbon Chromophores, Environ. Sci. Technol., 48, 12047-12055, https://doi.org/10.1021/es503432r, 2014.

Lee, B. H., Mohr, C., Lopez-Hilfiker, F. D., Lutz, A., Hallquist, M., Lee, L., Romer, P., Cohen, R. C., Iyer, S., Kurtén, T., Hu, W., Day, D. A., Campuzano-Jost, P., Jimenez, J. L., Xu, L., Ng, N. L., Guo, H., Weber, R. J., Wild, R. J., Brown, S. S., Koss, A., de Gouw, J., Olson, K., Goldstein, A. H., Seco, R., Kim, S., McAvey, K., Shepson, P. B., Starn, T., Baumann, K., Edgerton, E. S., Liu, J., Shilling, J. E., Miller, D. O., Brune, W., Schobesberger, S., D'Ambro, E. L., and Thornton, J. A.: Highly functionalized organic nitrates in the southeast United States: Contribution to secondary organic aerosol and reactive nitrogen budgets, P. Natl. Acad. Sci. USA, 113, 1516-1521, https://doi.org/10.1073/pnas.1508108113, 2016.

Li, S., Liu, D., Kong, S., Wu, Y., Hu, K., Zheng, H., Cheng, Y., Zheng, S., Jiang, X., Ding, S., Hu, D., Liu, Q., Tian, P., Zhao, D., and Sheng, J.: Evolution of source attributed organic aerosols and gases in a megacity of central China, Atmos. Chem. Phys., 22, 6937-6951, https://doi.org/10.5194/acp-22-6937-2022, 2022.

Li, Y., Chen, M., Wang, Y., Huang, T., Wang, G., Li, Z., Li, J., Meng, J., and Hou, Z.: Seasonal characteristics and provenance of organic aerosols in the urban atmosphere of Liaocheng in the North China Plain: Significant effect of biomass burning, Particuology, 75, 185-198, https://doi.org/10.1016/j.partic.2022.07.012, 2023.

Lin, P., Rincon, A. G., Kalberer, M., and Yu, J. Z.: Elemental Composition of HULIS in the Pearl River Delta Region, China: Results Inferred from Positive and Negative Electrospray High Resolution Mass Spectrometric Data, Environ. Sci.

706 Technol., 46, 7454-7462, https://doi.org/10.1021/es300285d, 2012.

707   Lin, X., Xu, Y., Zhu, R.-G., Xiao, H.-W., and Xiao, H.-Y.: Proteinaceous Matter in

708 $PM_{2.5}$ in Suburban Guiyang, Southwestern China: Decreased Importance in Long-

709 Range Transport and Atmospheric Degradation, J. Geophys. Res.-Atmos., 128,

710 e2023JD038516, https://doi.org/10.1029/2023JD038516, 2023.

711   Liu, T., Xu, Y., Sun, Q.-B., Xiao, H.-W., Zhu, R.-G., Li, C.-X., Li, Z.-Y., Zhang,

712 K.-Q., Sun, C.-X., and Xiao, H.-Y.: Characteristics, Origins, and Atmospheric

713 Processes of Amines in Fine Aerosol Particles in Winter in China, J. Geophys. Res.-

714 Atmos., 128, e2023JD038974, https://doi.org/10.1029/2023JD038974, 2023.

715   Liu, T., Hong, Y., Li, M., Xu, L., Chen, J., Bian, Y., Yang, C., Dan, Y., Zhang, Y.,

716 Xue, L., Zhao, M., Huang, Z., and Wang, H.: Atmospheric oxidation capacity and ozone

717 pollution mechanism in a coastal city of southeastern China: analysis of a typical

718 photochemical episode by an observation-based model, Atmos. Chem. Phys., 22, 2173-

719 2190, https://doi.org/10.5194/acp-22-2173-2022, 2022.

720   Ma, L., Guzman, C., Niedek, C., Tran, T., Zhang, Q., and Anastasio, C.: Kinetics

721 and Mass Yields of Aqueous Secondary Organic Aerosol from Highly Substituted

722 Phenols Reacting with a Triplet Excited State, Environ. Sci. Technol., 55, 5772-5781,

723 https://doi.org/10.1021/acs.est.1c00575, 2021.

724   Merder, J., Freund, J. A., Feudel, U., Hansen, C. T., Hawkes, J. A., Jacob, B.,

725 Klaproth, K., Niggemann, J., Noriega-Ortega, B. E., Osterholz, H., Rossel, P. E., Seidel,

726 M., Singer, G., Stubbins, A., Waska, H., and Dittmar, T.: ICBM-OCEAN: Processing

727 Ultrahigh-Resolution Mass Spectrometry Data of Complex Molecular Mixtures, Anal.

728 Chem., 92, 6832-6838, https://dx.doi.org/10.1021/acs.analchem.9b05659, 2020.

729 Nguyen, T. B., Bates, K. H., Crounse, J. D., Schwantes, R. H., Zhang, X.,

730 Kjaergaard, H. G., Surratt, J. D., Lin, P., Laskin, A., Seinfeld, J. H., and Wennberg, P.

731 O.: Mechanism of the hydroxyl radical oxidation of methacryloyl peroxynitrate (MPAN)

732 and its pathway toward secondary organic aerosol formation in the atmosphere, Phys.

733 Chem. Chem. Phys., 17, 17914-17926, https://doi.org/10.1039/C5CP02001H, 2015.

734 Perring, A. E., Pusede, S. E., and Cohen, R. C.: An Observational Perspective on

735 the Atmospheric Impacts of Alkyl and Multifunctional Nitrates on Ozone and

736 Secondary Organic Aerosol, Chem. Rev., 113, 5848-5870,

737 https://doi.org/10.1021/cr300520x, 2013.

738 Qiu, C. and Zhang, R.: Multiphase chemistry of atmospheric amines, Phys. Chem.

739 Chem. Phys., 15, 5738-5752, https://doi.org/10.1039/C3CP43446j, 2013.

740 Qizhi, M., Ying, L., Kang, W., and Qingfei, Z.: Spatio-Temporal Changes of

741 Population Density and Urbanization Pattern in China(2000–2010), China City Plan.

742 Rev., 25, 8-14, 2016.

743 Radzi Bin Abas, M., Rahman, N. A., Omar, N. Y. M. J., Maah, M. J., Abu Samah,

744 A., Oros, D. R., Otto, A., and Simoneit, B. R. T.: Organic composition of aerosol

745 particulate matter during a haze episode in Kuala Lumpur, Malaysia, Atmos. Environ.,

746 38, 4223-4241, https://doi.org/10.1016/j.atmosenv.2004.01.048, 2004.

747 Ren, Y., Wang, G., Wu, C., Wang, J., Li, J., Zhang, L., Han, Y., Liu, L., Cao, C.,

748 Cao, J., He, Q., and Liu, X.: Changes in concentration, composition and source

749 contribution of atmospheric organic aerosols by shifting coal to natural gas in Urumqi,

Atmos. Environ., 148, 306-315, https://doi.org/10.1016/j.atmosenv.2016.10.053, 2017.

Rollins, A. W., Browne, E. C., Min, K.-E., Pusede, S. E., Wooldridge, P. J., Gentner, D. R., Goldstein, A. H., Liu, S., Day, D. A., Russell, L. M., and Cohen, R. C.: Evidence for NO_x Control over Nighttime SOA Formation, Science, 337, 1210-1212, https://doi.org/10.1126/science.1221520, 2012.

Salvador, C. M. G., Tang, R., Priestley, M., Li, L., Tsiligiannis, E., Le Breton, M., Zhu, W., Zeng, L., Wang, H., Yu, Y., Hu, M., Guo, S., and Hallquist, M.: Ambient nitro-aromatic compounds – biomass burning versus secondary formation in rural China, Atmos. Chem. Phys., 21, 1389-1406, https://doi.org/10.5194/acp-21-1389-2021, 2021.

Samy, S. and Hays, M. D.: Quantitative LC–MS for water-soluble heterocyclic amines in fine aerosols ($PM_{2.5}$) at Duke Forest, USA, Atmos. Environ., 72, 77-80, https://doi.org/10.1016/j.atmosenv.2013.02.032, 2013.

Schauer, J. J., Kleeman, M. J., Cass, G. R., and Simoneit, B. R. T.: Measurement of Emissions from Air Pollution Sources. 1. C_1 through C_{29} Organic Compounds from Meat Charbroiling, Environ. Sci. Technol., 33, 1566-1577, https://doi.org/10.1021/es980076j, 1999.

Seinfeld, J. H., Bretherton, C., Carslaw, K. S., Coe, H., DeMott, P. J., Dunlea, E. J., Feingold, G., Ghan, S., Guenther, A. B., Kahn, R., Kraucunas, I., Kreidenweis, S. M., Molina, M. J., Nenes, A., Penner, J. E., Prather, K. A., Ramanathan, V., Ramaswamy, V., Rasch, P. J., Ravishankara, A. R., Rosenfeld, D., Stephens, G., and Wood, R.: Improving our fundamental understanding of the role of aerosol−cloud interactions in the climate system, P. Natl. Acad. Sci. USA, 113, 5781-5790,

772 https://doi.org/10.1073/pnas.1514043113, 2016.

773 Simoneit, B. R. T., Rushdi, A. I., bin Abas, M. R., and Didyk, B. M.: Alkyl Amides

774 and Nitriles as Novel Tracers for Biomass Burning, Environ. Sci. Technol., 37, 16-21,

775 https://doi.org/10.1021/es020811y, 2003.

776 Smith, J. D., Sio, V., Yu, L., Zhang, Q., and Anastasio, C.: Secondary Organic

777 Aerosol Production from Aqueous Reactions of Atmospheric Phenols with an Organic

778 Triplet Excited State, Environ. Sci. Technol., 48, 1049-1057,

779 https://doi.org/10.1021/es4045715, 2014.

780 Song, J., Li, M., Jiang, B., Wei, S., Fan, X., and Peng, P. a.: Molecular

781 Characterization of Water-Soluble Humic like Substances in Smoke Particles Emitted

782 from Combustion of Biomass Materials and Coal Using Ultrahigh-Resolution

783 Electrospray Ionization Fourier Transform Ion Cyclotron Resonance Mass

784 Spectrometry, Environ. Sci. Technol., 52, 2575-2585,

785 https://doi.org/10.1021/acs.est.7b06126, 2018.

786 Song, J., Li, M., Zou, C., Cao, T., Fan, X., Jiang, B., Yu, Z., Jia, W., and Peng, P.

787 a.: Molecular Characterization of Nitrogen-Containing Compounds in Humic-like

788 Substances Emitted from Biomass Burning and Coal Combustion, Environ. Sci.

789 Technol., 56, 119-130, https://doi.org/10.1021/acs.est.1c04451, 2022.

790 Stolzenburg, D., Fischer, L., Vogel, A. L., Heinritzi, M., Schervish, M., Simon, M.,

791 Wagner, A. C., Dada, L., Ahonen, L. R., Amorim, A., Baccarini, A., Bauer, P. S.,

792 Baumgartner, B., Bergen, A., Bianchi, F., Breitenlechner, M., Brilke, S., Buenrostro

793 Mazon, S., Chen, D., Dias, A., Draper, D. C., Duplissy, J., El Haddad, I., Finkenzeller,

H., Frege, C., Fuchs, C., Garmash, O., Gordon, H., He, X., Helm, J., Hofbauer, V.,

Hoyle, C. R., Kim, C., Kirkby, J., Kontkanen, J., Kürten, A., Lampilahti, J., Lawler, M.,

Lehtipalo, K., Leiminger, M., Mai, H., Mathot, S., Mentler, B., Molteni, U., Nie, W.,

Nieminen, T., Nowak, J. B., Ojdanic, A., Onnela, A., Passananti, M., Petäjä, T.,

Quéléver, L. L. J., Rissanen, M. P., Sarnela, N., Schallhart, S., Tauber, C., Tomé, A.,

Wagner, R., Wang, M., Weitz, L., Wimmer, D., Xiao, M., Yan, C., Ye, P., Zha, Q.,

Baltensperger, U., Curtius, J., Dommen, J., Flagan, R. C., Kulmala, M., Smith, J. N.,

Worsnop, D. R., Hansel, A., Donahue, N. M., and Winkler, P. M.: Rapid growth of

organic aerosol nanoparticles over a wide tropospheric temperature range, P. Natl. Acad.

Sci. USA, 115, 9122-9127, https://doi.org/10.1073/pnas.1807604115, 2018.

Su, S., Xie, Q., Lang, Y., Cao, D., Xu, Y., Chen, J., Chen, S., Hu, W., Qi, Y., Pan,

X., Sun, Y., Wang, Z., Liu, C.-Q., Jiang, G., and Fu, P.: High Molecular Diversity of

Organic Nitrogen in Urban Snow in North China, Environ. Sci. Technol., 55, 4344-

4356, https://dx.doi.org/10.1021/acs.est.0c06851, 2021.

Surratt, J. D., Chan, A. W. H., Eddingsaas, N. C., Chan, M., Loza, C. L., Kwan, A.

J., Hersey, S. P., Flagan, R. C., Wennberg, P. O., and Seinfeld, J. H.: Reactive

intermediates revealed in secondary organic aerosol formation from isoprene, P. Natl.

Acad. Sci. USA, 107, 6640-6645, https://doi.org/10.1073/pnas.0911114107, 2010.

Tomsche, L., Piel, F., Mikoviny, T., Nielsen, C. J., Guo, H., Campuzano-Jost, P.,

Nault, B. A., Schueneman, M. K., Jimenez, J. L., Halliday, H., Diskin, G., DiGangi, J.

P., Nowak, J. B., Wiggins, E. B., Gargulinski, E., Soja, A. J., and Wisthaler, A.:

Measurement report: Emission factors of NH3 and NHx for wildfires and agricultural

fires in the United States, Atmos. Chem. Phys., 23, 2331-2343, https://doi.org/10.5194/acp-23-2331-2023, 2023.

W. Hogg, R. and T. Gillan, F.: Fatty acids, sterols and hydrocarbons in the leaves from eleven species of mangrove, Phytochemistry, 23, 93-97, https://doi.org/10.1016/0031-9422(84)83084-8, 1984.

Wan, X., Qin, F., Cui, F., Chen, W., Ding, H., and Li, C.: Correlation between the distribution of solar energy resources and the cloud cover in Xinjiang, IOP Conf. Ser.: Earth Environ. Sci., 675, 012060, https://doi.org/10.1088/1755-1315/675/1/012060, 2021.

Wang, H., Wang, Q., Gao, Y., Zhou, M., Jing, S., Qiao, L., Yuan, B., Huang, D., Huang, C., Lou, S., Yan, R., de Gouw, J. A., Zhang, X., Chen, J., Chen, C., Tao, S., An, J., and Li, Y.: Estimation of Secondary Organic Aerosol Formation During a Photochemical Smog Episode in Shanghai, China, J. Geophys. Res.-Atmos., 125, e2019JD032033, https://doi.org/10.1029/2019JD032033, 2020.

Wang, K., Huang, R.-J., Brueggemand, M., Zhang, Y., Yang, L., Ni, H., Guo, J., Wang, M., Han, J., Bilde, M., Glasius, M., and Hoffmann, T.: Urban organic aerosol composition in eastern China differs from north to south: molecular insight from a liquid chromatography-mass spectrometry (Orbitrap) study, Atmos. Chem. Phys., 21, 9089-9104, https://doi.org/10.5194/acp-21-9089-2021, 2021a.

Wang, L., Zhang, K., Huang, W., Han, W., and Tian, C.-Y.: Seed oil content and fatty acid composition of annual halophyte Suaeda acuminata: A comparative study on dimorphic seeds, Afr. J. Biotechnol., 10, 19106-19108,

838   https://doi.org/10.5897/ajb11.2597, 2011.

839   Wang, Q., Shao, M., Zhang, Y., Wei, Y., Hu, M., and Guo, S.: Source

840   apportionment of fine organic aerosols in Beijing, Atmos. Chem. Phys., 9, 8573-8585,

841   https://doi.org/10.5194/acp-9-8573-2009, 2009.

842   Wang, X., Hayeck, N., Brüggemann, M., Yao, L., Chen, H., Zhang, C., Emmelin,

843   C., Chen, J., George, C., and Wang, L.: Chemical Characteristics of Organic Aerosols

844   in Shanghai: A Study by Ultrahigh-Performance Liquid Chromatography Coupled With

845   Orbitrap Mass Spectrometry, J. Geophys. Res.-Atmos., 122, 11,703-711,722,

846   https://doi.org/10.1002/2017JD026930, 2017a.

847   Wang, X., Shen, Z., Liu, F., Lu, D., Tao, J., Lei, Y., Zhang, Q., Zeng, Y., Xu, H.,

848   Wu, Y., Zhang, R., and Cao, J.: Saccharides in summer and winter $PM_{2.5}$ over Xi'an,

849   Northwestern China: Sources, and yearly variations of biomass burning contribution to

850    $PM_{2.5}$, Atmos. Res., 214, 410-417, https://doi.org/10.1016/j.atmosres.2018.08.024,

851   2018.

852   Wang, Y., Zhao, Y., Li, Z., Li, C., Yan, N., and Xiao, H.: Importance of Hydroxyl

853   Radical Chemistry in Isoprene Suppression of Particle Formation from α-Pinene

854   Ozonolysis,   ACS   Earth   Space   Chem.,   5,   487-499,

855   https://doi.org/10.1021/acsearthspacechem.0c00294, 2021b.

856   Wang, Y., Hu, M., Lin, P., Guo, Q., Wu, Z., Li, M., Zeng, L., Song, Y., Zeng, L.,

857   Wu, Y., Guo, S., Huang, X., and He, L.: Molecular Characterization of Nitrogen-

858   Containing Organic Compounds in Humic-like Substances Emitted from Straw

859   Residue   Burning,   Environ.   Sci.   Technol.,   51,   5951-5961,

860 https://doi.org/10.1021/acs.est.7b00248, 2017b.

861   Wang, Y., Hu, M., Hu, W., Zheng, J., Niu, H., Fang, X., Xu, N., Wu, Z., Guo, S.,

862 Wu, Y., Chen, W., Lu, S., Shao, M., Xie, S., Luo, B., and Zhang, Y.: Secondary

863 Formation of Aerosols Under Typical High-Humidity Conditions in Wintertime

864 Sichuan Basin, China: A Contrast to the North China Plain, J. Geophys. Res.-Atmos.,

865 126, e2021JD034560, https://doi.org/10.1029/2021JD034560, 2021c.

866   Xie, Q., Su, S., Chen, S., Xu, Y., Cao, D., Chen, J., Ren, L., Yue, S., Zhao, W., Sun,

867 Y., Wang, Z., Tong, H., Su, H., Cheng, Y., Kawamura, K., Jiang, G., Liu, C. Q., and Fu,

868 P.: Molecular characterization of firework-related urban aerosols using Fourier

869 transform ion cyclotron resonance mass spectrometry, Atmos. Chem. Phys., 20, 6803-

870 6820, https://doi.org/10.5194/acp-20-6803-2020, 2020.

871   Xu, Y. and Xiao, H.: Concentrations and nitrogen isotope compositions of free

872 amino acids in Pinus massoniana (Lamb.) needles of different ages as indicators of

873 atmospheric nitrogen pollution, Atmos. Environ., 164, 348-359,

874 https://doi.org/10.1016/j.atmosenv.2017.06.024, 2017.

875   Xu, Y., Lin, Z., and Wu, C.: Spatiotemporal Variation of the Burned Area and Its

876 Relationship with Climatic Factors in Central Kazakhstan, Remote Sens., 13, 313,

877 https://doi.org/10.3390/rs13020313, 2021.

878   Xu, Y., Dong, X.-N., Xiao, H.-Y., He, C., and Wu, D.-S.: Water-Insoluble

879 Components in Rainwater in Suburban Guiyang, Southwestern China: A Potential

880 Contributor to Dissolved Organic Carbon, J. Geophys. Res.-Atmos., 127,

881 e2022JD037721, https://doi.org/10.1029/2022JD037721, 2022a.

882   Xu, Y., Dong, X.-N., Xiao, H.-Y., Zhou, J.-X., and Wu, D.-S.: Proteinaceous

883   Matter and Liquid Water in Fine Aerosols in Nanchang, Eastern China: Seasonal

884   Variations, Sources, and Potential Connections, J. Geophys. Res.-Atmos., 127,

885   e2022JD036589, https://doi.org/10.1029/2022JD036589, 2022b.

886   Xu, Y., Dong, X. N., He, C., Wu, D. S., Xiao, H. W., and Xiao, H. Y.: Mist cannon

887   trucks can exacerbate the formation of water-soluble organic aerosol and $PM_{2.5}$

888   pollution in the road environment, Atmos. Chem. Phys., 23, 6775-6788,

889   https://doi.org/10.5194/acp-23-6775-2023, 2023.

890   Xu, Y., Miyazaki, Y., Tachibana, E., Sato, K., Ramasamy, S., Mochizuki, T.,

891   Sadanaga, Y., Nakashima, Y., Sakamoto, Y., Matsuda, K., and Kajii, Y.: Aerosol Liquid

892   Water Promotes the Formation of Water-Soluble Organic Nitrogen in Submicrometer

893   Aerosols in a Suburban Forest, Environ. Sci. Technol., 54, 1406-1414,

894   https://dx.doi.org/10.1021/acs.est.9b05849, 2020.

895   Yang, T., Xu, Y., Ye, Q., Ma, Y. J., Wang, Y. C., Yu, J. Z., Duan, Y. S., Li, C. X.,

896   Xiao, H. W., Li, Z. Y., Zhao, Y., and Xiao, H. Y.: Spatial and diurnal variations of aerosol

897   organosulfates in summertime Shanghai, China: potential influence of photochemical

898   processes and anthropogenic sulfate pollution, Atmos. Chem. Phys., 23, 13433-13450,

899   https://doi.org/10.5194/acp-23-13433-2023, 2023.

900   Zahardis, J., Geddes, S., and Petrucci, G. A.: The ozonolysis of primary aliphatic

901   amines in fine particles, Atmos. Chem. Phys., 8, 1181-1194,

902   https://doi.org/10.5194/acp-8-1181-2008, 2008.

903   Zarzana, K. J., De Haan, D. O., Freedman, M. A., Hasenkopf, C. A., and Tolbert,

M. A.: Optical Properties of the Products of α-Dicarbonyl and Amine Reactions in Simulated Cloud Droplets, Environ. Sci. Technol., 46, 4845-4851, https://doi.org/10.1021/es2040152, 2012.

Zeng, Y., Ning, Y., Shen, Z., Zhang, L., Zhang, T., Lei, Y., Zhang, Q., Li, G., Xu, H., Ho, S. S. H., and Cao, J.: The Roles of N, S, and O in Molecular Absorption Features of Brown Carbon in PM2.5 in a Typical Semi-Arid Megacity in Northwestern China, J. Geophys. Res.-Atmos., 126, e2021JD034791, https://doi.org/10.1029/2021JD034791, 2021.

Zeng, Y., Shen, Z., Takahama, S., Zhang, L., Zhang, T., Lei, Y., Zhang, Q., Xu, H., Ning, Y., Huang, Y., Cao, J., and Rudolf, H.: Molecular Absorption and Evolution Mechanisms of PM2.5 Brown Carbon Revealed by Electrospray Ionization Fourier Transform–Ion Cyclotron Resonance Mass Spectrometry During a Severe Winter Pollution Episode in Xi'an, China, Geophys. Res. Lett., 47, e2020GL087977, https://doi.org/10.1029/2020GL087977, 2020.

Zhang, B., Shen, Z., He, K., Sun, J., Huang, S., Xu, H., Li, J., Ho, S. S. H., and Cao, J.-j.: Insight into the Primary and Secondary Particle-Bound Methoxyphenols and Nitroaromatic Compound Emissions from Solid Fuel Combustion and the Updated Source Tracers, Environ. Sci. Technol., 57, 14280-14288, 10.1021/acs.est.3c04370, 2023.

Zhang, Q., Jimenez, J. L., Canagaratna, M. R., Allan, J. D., Coe, H., Ulbrich, I., Alfarra, M. R., Takami, A., Middlebrook, A. M., Sun, Y. L., Dzepina, K., Dunlea, E., Docherty, K., DeCarlo, P. F., Salcedo, D., Onasch, T., Jayne, J. T., Miyoshi, T., Shimono,

A., Hatakeyama, S., Takegawa, N., Kondo, Y., Schneider, J., Drewnick, F., Borrmann, S., Weimer, S., Demerjian, K., Williams, P., Bower, K., Bahreini, R., Cottrell, L., Griffin, R. J., Rautiainen, J., Sun, J. Y., Zhang, Y. M., and Worsnop, D. R.: Ubiquity and dominance of oxygenated species in organic aerosols in anthropogenically-influenced Northern Hemisphere midlatitudes, Geophys. Res. Lett., 34, https://doi.org/10.1029/2007GL029979, 2007.

Zhang, T., Shen, Z., Huang, S., Lei, Y., Zeng, Y., Sun, J., Zhang, Q., Ho, S. S. H., Xu, H., and Cao, J.: Optical properties, molecular characterizations, and oxidative potentials of different polarity levels of water-soluble organic matters in winter PM2.5 in six China's megacities, Sci. Total Environ., 853, 158600, https://doi.org/10.1016/j.scitotenv.2022.158600, 2022.

Zhao, Y., Hu, M., Slanina, S., and Zhang, Y.: Chemical Compositions of Fine Particulate Organic Matter Emitted from Chinese Cooking, Environ. Sci. Technol., 41, 99-105, https://doi.org/10.1021/es0614518, 2007.

Zhong, S., Chen, S., Deng, J., Fan, Y., Zhang, Q., Xie, Q., Qi, Y., Hu, W., Wu, L., Li, X., Pavuluri, C. M., Zhu, J., Wang, X., Liu, D., Pan, X., Sun, Y., Wang, Z., Xu, Y., Tong, H., Su, H., Cheng, Y., Kawamura, K., and Fu, P.: Impact of biogenic secondary organic aerosol (SOA) loading on the molecular composition of wintertime $PM_{2.5}$ in urban Tianjin: an insight from Fourier transform ion cyclotron resonance mass spectrometry, Atmos. Chem. Phys., 23, 2061-2077, https://doi.org/10.5194/acp-23-2061-2023, 2023.

Zhou, S., Guo, F., Chao, C.-Y., Yoon, S., Alvarez, S. L., Shrestha, S., Flynn, J. H.,

III, Usenko, S., Sheesley, R. J., and Griffin, R. J.: Marine Submicron Aerosols from the Gulf of Mexico: Polluted and Acidic with Rapid Production of Sulfate and Organosulfates, Environ. Sci. Technol., 57, 5149-5159, https://doi.org/10.1021/acs.est.2c05469, 2023.

Zou, C., Cao, T., Li, M., Song, J., Jiang, B., Jia, W., Li, J., Ding, X., Yu, Z., Zhang, G., and Peng, P.: Measurement report: Changes in light absorption and molecular composition of water-soluble humic-like substances during a winter haze bloom-decay process in Guangzhou, China, Atmos. Chem. Phys., 23, 963-979, https://doi.org/10.5194/acp-23-963-2023, 2023.

958 **Figure 1.**
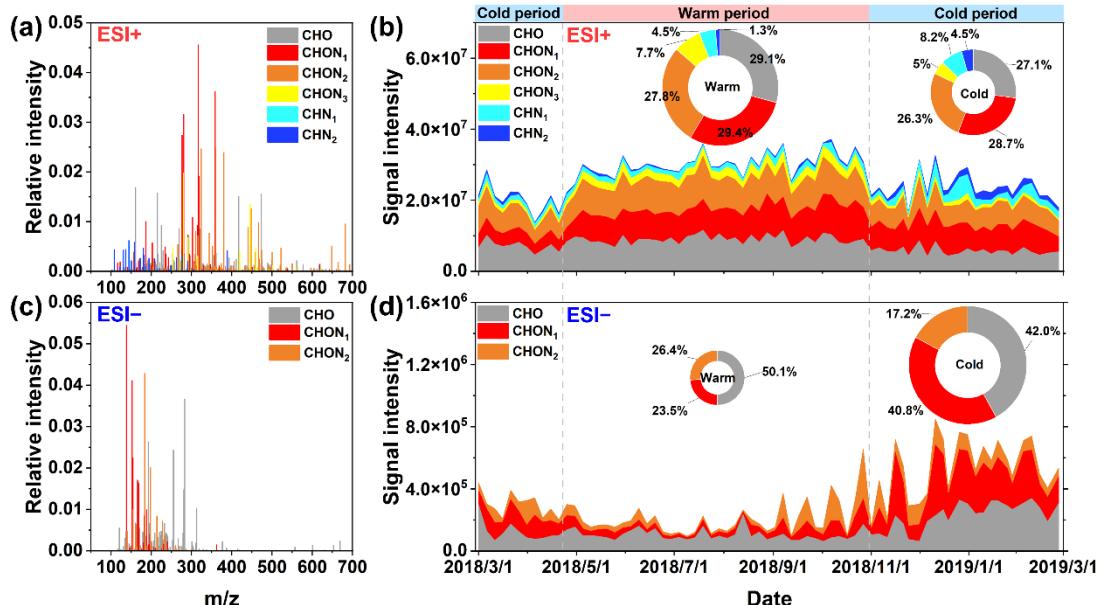
959

960 **Figure 1.** The reconstructed mass spectrum distribution of the detected species in PM$_{2.5}$

961 in (**a**) ESI+ and (**c**) ESI− modes during the whole campaign. Temporal variations in the

962 fractional distribution of classified compounds in (**b**) ESI+ and (**d**) ESI− modes. The

963 ring diagrams inside the panel show the signal intensity fractions of classified

964 compounds, the size of which is proportional to the total signal intensity of all species

965 detected in PM$_{2.5}$ in different periods.

966

967

968

969 **Figure 2.**
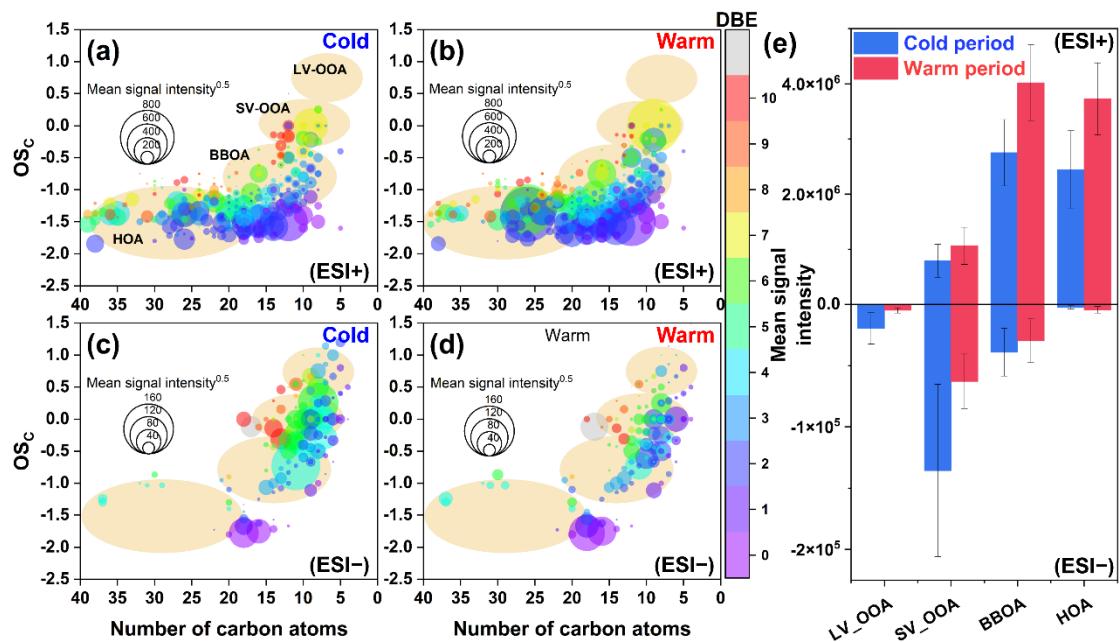
970

971 **Figure 2.** OSc values of CHO molecules detected in (**a** and **b**) ESI+ and (**c** and **d**) ESI−

972 modes in PM$_{2.5}$ collected from different periods (cold vs. warm). The size and color of

973 the circle indicate the mean signal intensity and DBE value of compounds, respectively.

974 The light-orange background indicates the areas of LV-OOA, SV-OOA, BBOA, and

975 HOA (Kroll et al., 2011), according to which (**e**) the mean signal intensity of classified

976 compounds was calculated for samples from different periods.

977

978

979

980
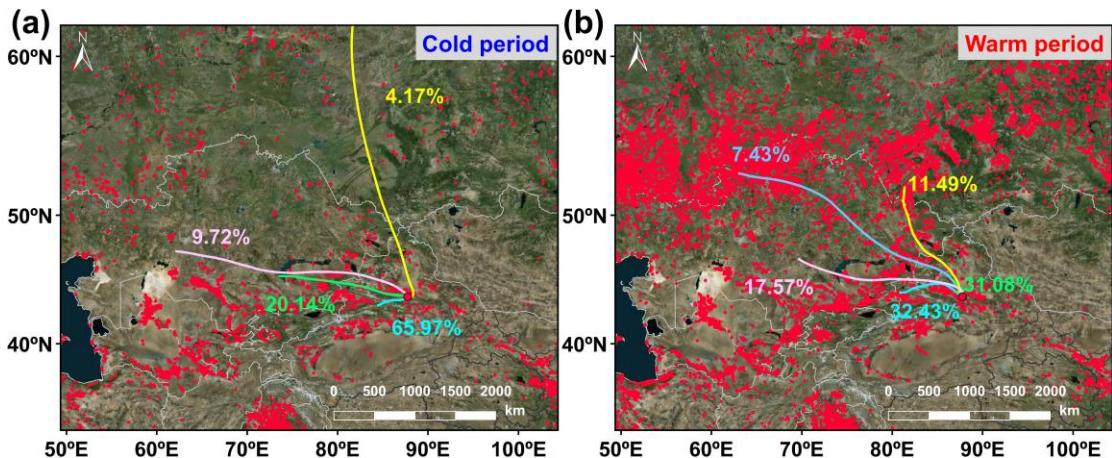
Figure 3

Figure 3. The 3-day (72 h) back trajectories illustrating the typical air mass flows to the study site during the (a) warm and (b) cool periods. Fire spots were shown in red, which was created based on NASA active fire data (VIIRS 375 m, https://firms.modaps.eosdis.nasa.gov/active_fire/). The map was derived from ©MeteoInfoMap (version 3.6.2) (Chinese Academy of Meteorological Sciences, China).

992 **Figure 4.**
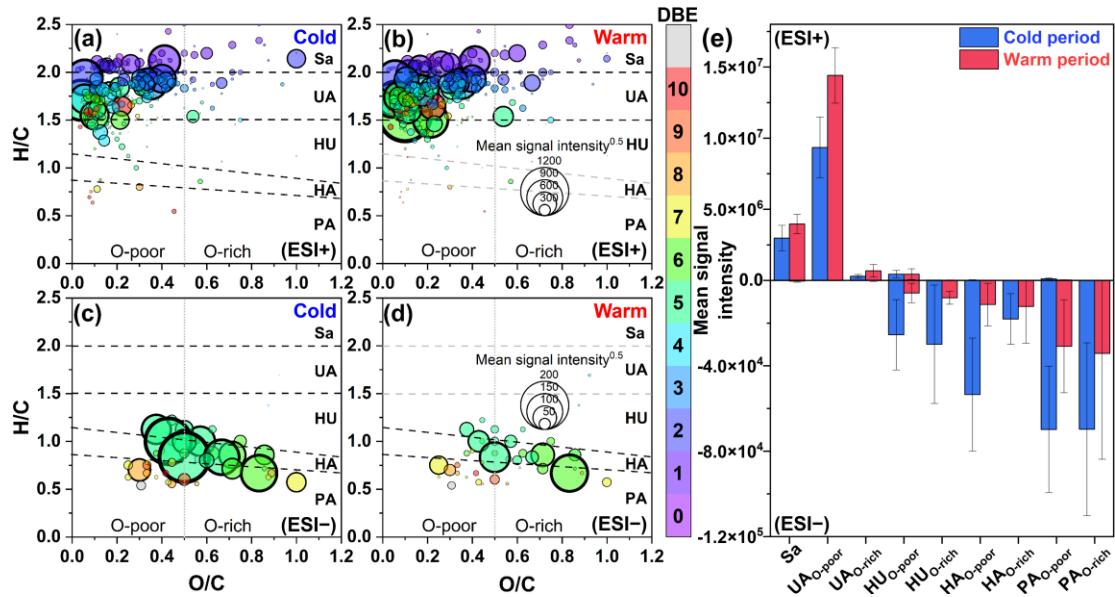
993

994 **Figure 4.** Van Krevelen diagrams of CHON molecules detected in (**a** and **b**) ESI+ and

995 (**c** and **d**) ESI− modes in PM$_{2.5}$ collected from different periods (cold vs. warm). The

996 subgroups in the panel include saturated-like (Sa), unsaturated aliphatic-like (UA),

997 highly unsaturated-like (HU), highly aromatic-like (HA), and polycyclic aromatic-like

998 (PA) compounds, further distinguishing between oxygen-poor and oxygen-rich

999 compounds with an oxygen to carbon ratio of 0.5. The size and color of the circle

1000 indicate the mean signal intensity and DBE value of compounds, respectively. The (**e**)

1001 mean signal intensity of classified compounds was calculated for samples from

1002 different periods.

1003

1004

1005

1006

1007 **Figure 5.**

1008
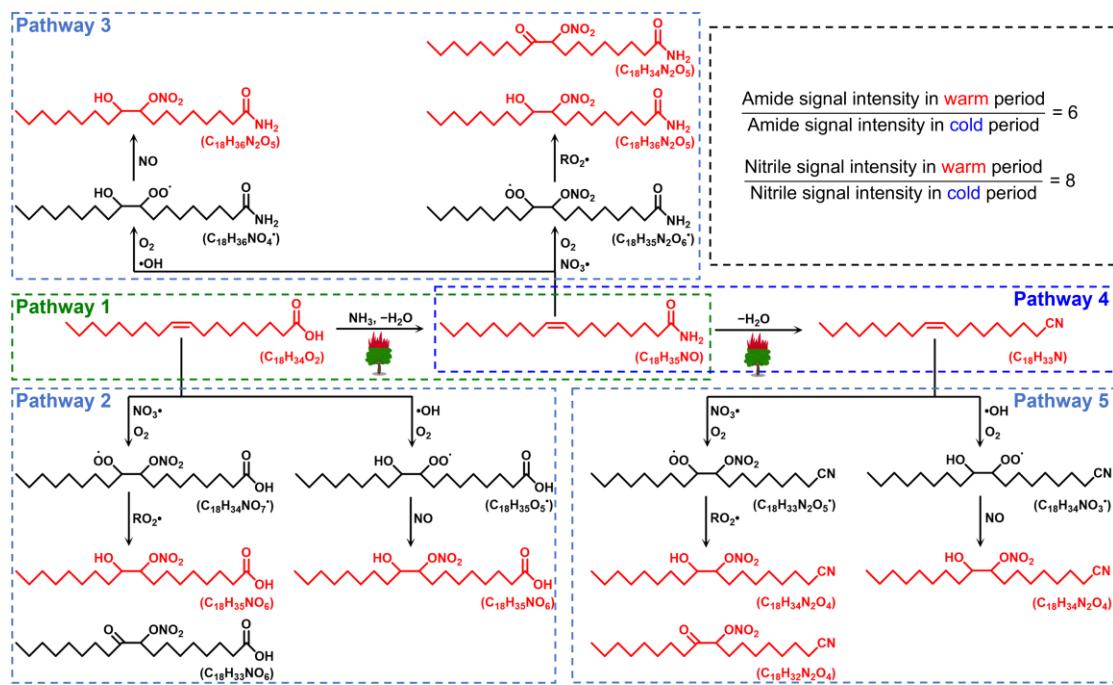
1009 **Figure 5.** Proposed pathways for the reactions of carboxylic acids (oleic acid as a

1010 representative) with reactive nitrogen and atmospheric oxides to form the observed

1011 NOCs in PM$_{2.5}$ under the influence of the high temperature generated during wildfires

1012 or forest fires. Compounds observed in PM$_{2.5}$ were shown in red.

1013

1014   **Figure 6.**
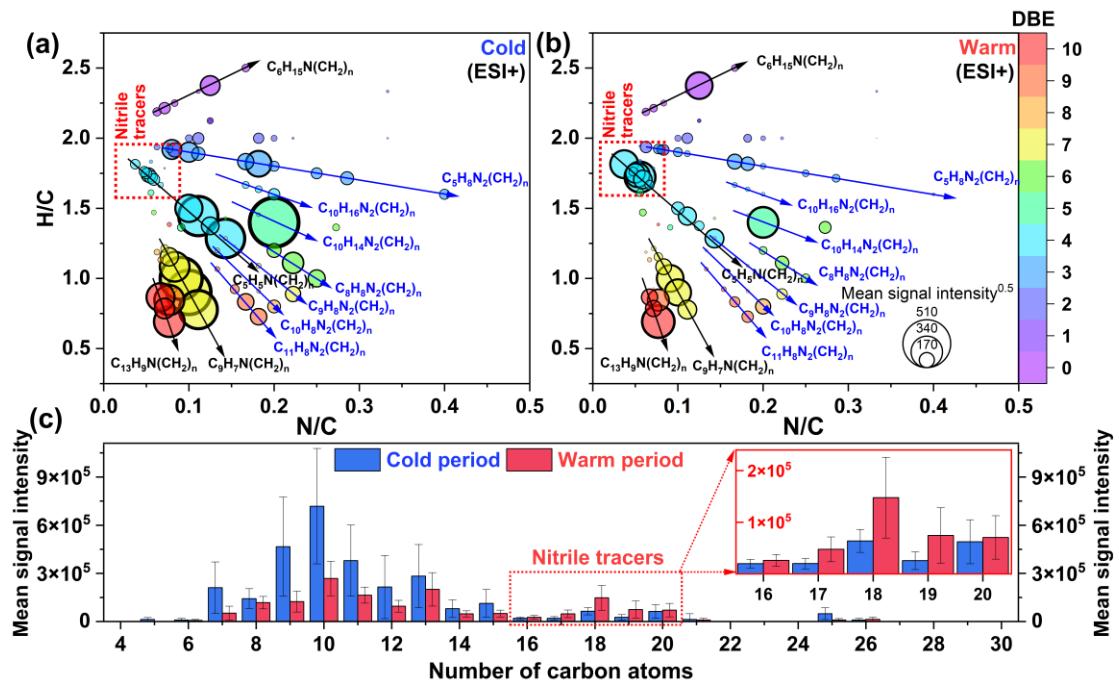
1015

1016   **Figure 6.** Van Krevelen diagrams of CHN molecules detected in PM$_{2.5}$ collected from

1017   the (**a**) cold and (**b**) warm periods. The size and color of the circle indicate the mean

1018   signal intensity and DBE value of compounds, respectively. The mean signal intensity

1019   distributions of (**c**) carbon atoms in CHN molecules detected in PM$_{2.5}$ collected from

1020   the cold and warm periods

1021

1022 **Figure 7.**
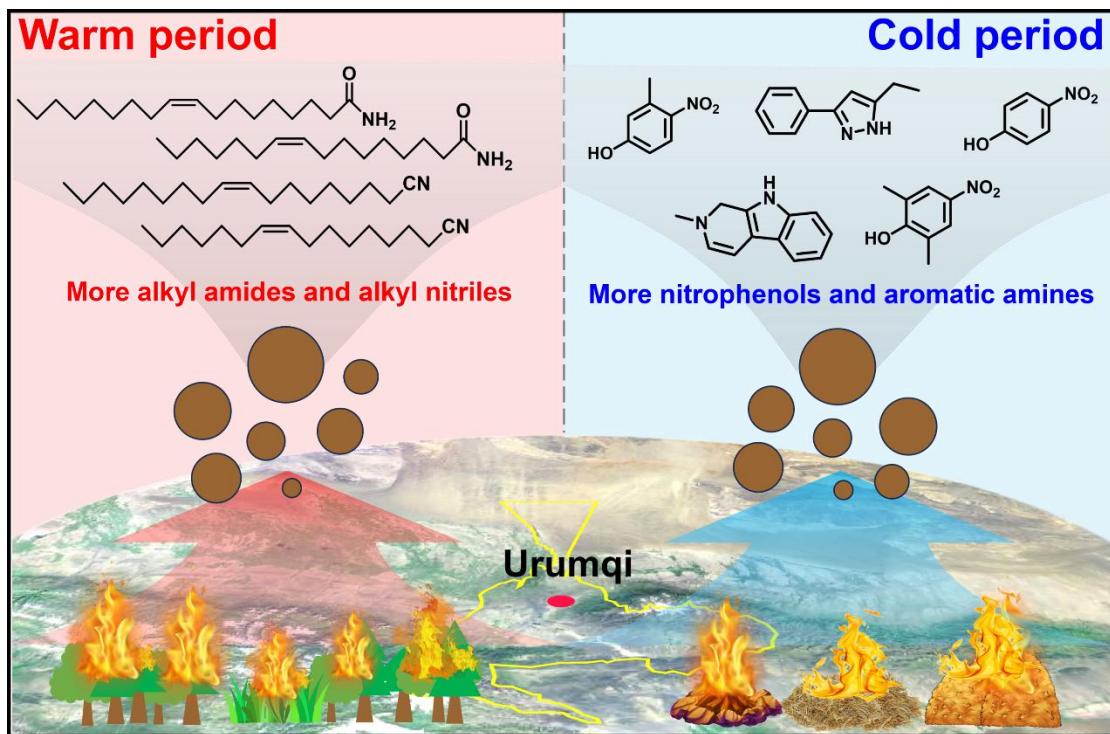
1023

1024 **Figure 7.** Conceptual picture showing the differential impacts of combustion of fresh

1025 and old-age biomass materials on aerosol NOCs in suburban Urumqi. The map was

1026 derived from ©Baidu Maps (BIDU, China).